

**TARGET SIZE DEPENDENCE OF DISRUPTION THRESHOLD: COLLISIONAL FRAGMENTATION EXPERIMENTS OF MILLIMETER SCALE ROCKS.** S. Takasawa<sup>1</sup>, A. M. Nakamura<sup>1</sup> and K. Sangen<sup>1</sup>,  
<sup>1</sup>Graduate School of Science, Kobe University, 1-1 Rokkodai, Nada-ku, Kobe, Japan (susumu@stu.kobe-u.ac.jp).

**Introduction:** Collisional disruption plays an important role in formation and evolution processes of dusts in the asteroid main belt and debris discs of young stellar objects. In collision cascades, bodies become smaller and smaller by successive collisions, and dust particles are supplied continuously. Size distribution for the circumstellar dust particles in collision cascades is estimated to be affected by target size dependence of the disruption threshold [1]. Catastrophic disruption threshold ( $Q^*$ ) is defined as the specific energy when catastrophic destruction of the target of mass  $M_T$  occurs, that is, the largest fragment mass  $m_L$  is the half of the original mass, i.e.,  $m_L/M_T = 0.5$ . It is theoretically expected and shown by numerical simulations that the disruption threshold is dependent on event size scale, and decreases with increasing target size in strength-dominated regime. This trend was confirmed by laboratory collisional experiments of granite targets of size between 1.9 and 34.4 cm in diameter, performed under the impact conditions designed to examine target size effects [2]. However, size dependence of the disruption threshold of targets smaller than  $\sim$ cm in size has not been studied by laboratory collisional experiments so far. In this study, we conducted collisional disruption experiments of pyrophyllite targets down to 1 mm in size in order to examine whether size dependence of the disruption threshold can be extrapolated into smaller size scale. Moreover, we measured the static tensile strengths of pyrophyllite specimens in order to discuss difference of the dependence on sample size between static strength and collisional disruption threshold.

**Experiments:** Targets were very homogeneous cube-shaped pyrophyllites. We defined three different experimental groups according to collisional size scale. In group (A), projectiles were aluminum cylinder, 15 mm in diameter and 20 mm in length. The targets were from 19.4 to 45.1 mm on a side. We used a powder gun at Kobe University, and launched the projectiles at velocities from 168 to 391 m/s. In group (B), soda-lime glass spheres of 3.2 mm in diameter were shot into the targets of size from 2.8 to 7.3 mm on a side at velocity of about 245 m/s. In group (C), aluminum spheres of 1.0 mm in diameter were shot into the targets of size from 1.0 to 1.9 mm on a side at velocity of approximately 210 m/s. The impact experiments in both groups (B) and (C) were performed using a small helium gas-gun at Kobe University. In group (C), the projectile was accelerated with a polycarbonate sabot of 3.0 mm in diameter which fit the gun barrel. The

sabot is stopped at the gun muzzle by a sabot-stopper, then only projectile was shot to the target. Projectile velocities were measured on images taken by a high-speed camera for groups (A) and (C). We expect a constant speed of projectiles of the experiments for group (B). Table 1 shows geometric average size of the targets ( $L_a$ ), ratio of the projectile mass to the target mass ( $M_p/M_T$ ), and impact velocities ( $v_i$ ). Collision conditions, i.e., the range of mass ratio and the impact velocity were approximately the same for the three groups. Therefore these conditions are appropriate to examine the target size dependence of the catastrophic disruption threshold.

Static tensile strengths of pyrophyllite specimens were measured by Brazilian test using a compressive testing machine installed at Kobe University. Disc-shaped specimens of 10 mm in diameter and 5 mm in thickness were tested seventeen times, and the Weibull parameter ( $\phi$ ) was determined [3]. We derived the size dependence of the static strength of pyrophyllite specimens.

**Table 1.** Summary of experimental conditions.

Group	$L_a$ [mm]	$M_p/M_T$	$v_i$ [m/s]
A	32.8	0.04~0.5	170~390
B	4.4	0.04~0.7	245
C	1.6	0.04~0.5	210

**Results:** We plotted the mass of the largest fragment normalized by the original target mass ( $m_L/M_T$ ) against the projectile's kinetic energy per unit total mass of the system, that is  $M_p+M_T$ , where  $M_p$  is the projectile mass ( $Q$ ) in Figure 1. It is obvious that the data for each group shift to the right as the average target size decreases. The dashed line corresponds to the result of previous collisional experiments of  $\sim$ cm pyrophyllite targets [4] that matches the results of group (A). The values of  $Q^*$  for three groups are shown as a function of the target size in Figure 2. As shown in the Fig. 2,  $Q_s^*$  and the target size are expressed by a single power law down to about 1 mm. A regression fit represents a slope of -0.51, which results in a value of the Weibull parameter ( $\phi$ ) of pyrophyllite, 7.5. As for granite targets, the disruption threshold depends on the target size with a slope of -0.41, which corresponds to  $\phi = 8.9$  [2].

Figure 3 shows the cumulative probabilities ( $P$ ) of failure as a function of the applied tensile stress ( $\sigma$ )

based on Brazilian tests. We fitted the data with following equation,

$$P = 1 - \exp[-(\sigma/\sigma_0)^\varphi], \quad (1)$$

where  $\sigma_0$  is the characteristic stress [3]. We obtained a value of  $\varphi$  and  $\sigma_0$  for pyrophyllite material, 10.9 and 9.1 MPa, respectively. The value of  $\varphi$  for pyrophyllite material is larger than that of granite, 12.0 [2]. Both of the two experimental results indicate that the value of  $\varphi$  determined from the static strength measurements is larger than that determined from the dynamic collisional experiments.

A possible cause of the difference in the value of  $\varphi$  determined from the static strength measurements and the dynamic collisional experiments is considered due to the internal flaw-size distribution of granite whose slope gradually becomes steep with increasing flaw size [2]. We polished the surface of the pyrophyllite specimen and tried to observe the internal flaws under a scanning electron microscope (SEM). However, there is little evidence of flaw down to tens of  $\mu m$  on the SEM images.

**Discussion:** Mass distribution of circumstellar dust particles is denoted by  $n(m) \propto m^{-\beta}$ , where  $n(m)$  is differential number of body of mass  $m$ . When it is in collisional equilibrium cascades, the slope,  $\beta$ , can be written as  $\beta = (11+3p) / (6+3p)$ . The value of  $p$  is the slope of the size dependence of  $Q^*$ , that is,  $Q^* \propto M_T^p$  [1]. We found that  $p = -0.17$  for  $mm \sim cm$  scale pyrophyllite target. Assuming that this size dependence of  $Q^*$  can be extrapolated down to dust-sized range ( $\sim \mu m$ ), mass distribution for circumstellar dust particles in collisional cascades can be approximated as  $n(m) \propto m^{-1.9}$  using the average value of granite and pyrophyllite data obtained by laboratory collisional experiments. It is corresponding to  $n(a) \propto a^{-3.7}$ , where  $n(a)$  is differential number of size  $a$ . This slope is slightly steeper than that previously estimated, -3.5, on the assumption that  $Q^*$  is independent of masses of colliding bodies [5, 6].

**References:** [1] Kobayashi H. and Tanaka H. (2010) *Icarus*, 206, 735–746. [2] Housen K. R. and Holsapple K. A. (1999) *Icarus*, 142, 21–33. [3] Nakamura A. M., Michel P. and Setoh M. (2007) *J. Geophys. Res.*, 112, E02001. [4] Takagi Y., Mizutani H. and Kawakami S. (1984) *Icarus*, 59, 462–477. [5] Dohnanyi J. W. (1969) *J. Geophys. Res.*, 74, 2531–2554. [6] Tanaka H., Inaba S. and Nakazawa K. (1996) *Icarus*, 123, 450–455.

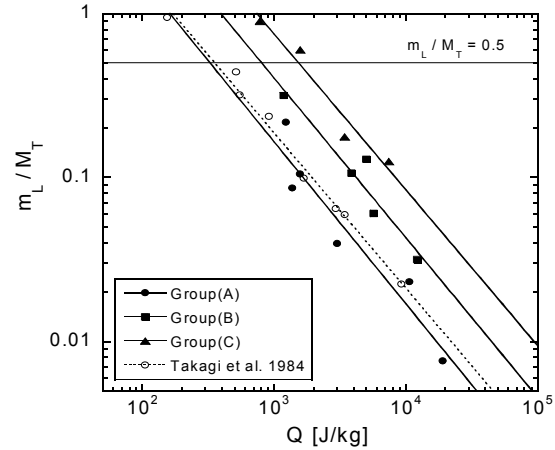


**Figure 1.** Specific kinetic energy of projectile ( $Q$ ) versus normalized mass of the largest fragment ( $m_L/M_T$ ). The dashed line corresponds to the result of previous collisional experiment of  $\sim cm$  pyrophyllite targets [3].

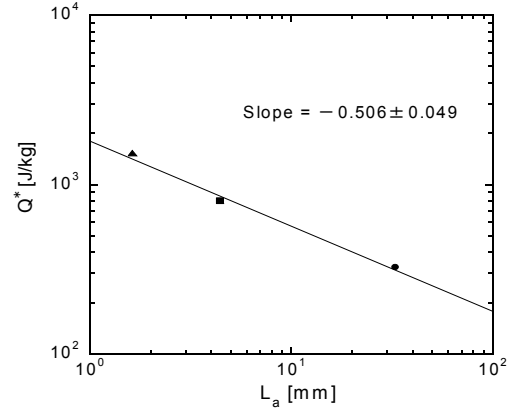


**Figure 2.** The power-law relationship between the disruption threshold ( $Q^*$ ) for each of the three groups and the average target size ( $L_a$ ).

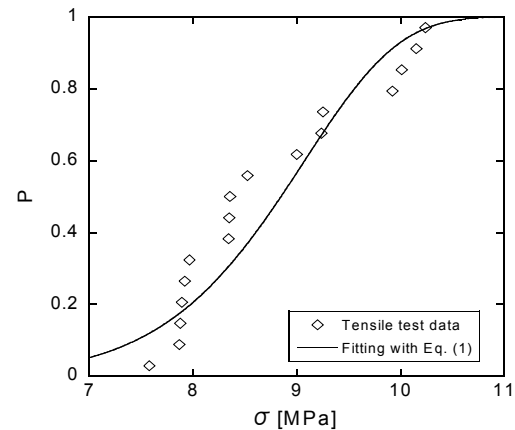


**Figure 3.** Failure probability ( $P$ ) as a function of the applied tensile stress ( $\sigma$ ). Diamond-shaped plots indicate the laboratory data, whereas the curve is indicative of the fitting with Eq. (1).